IJMRSETM

e-ISSN: 2395 - 7639

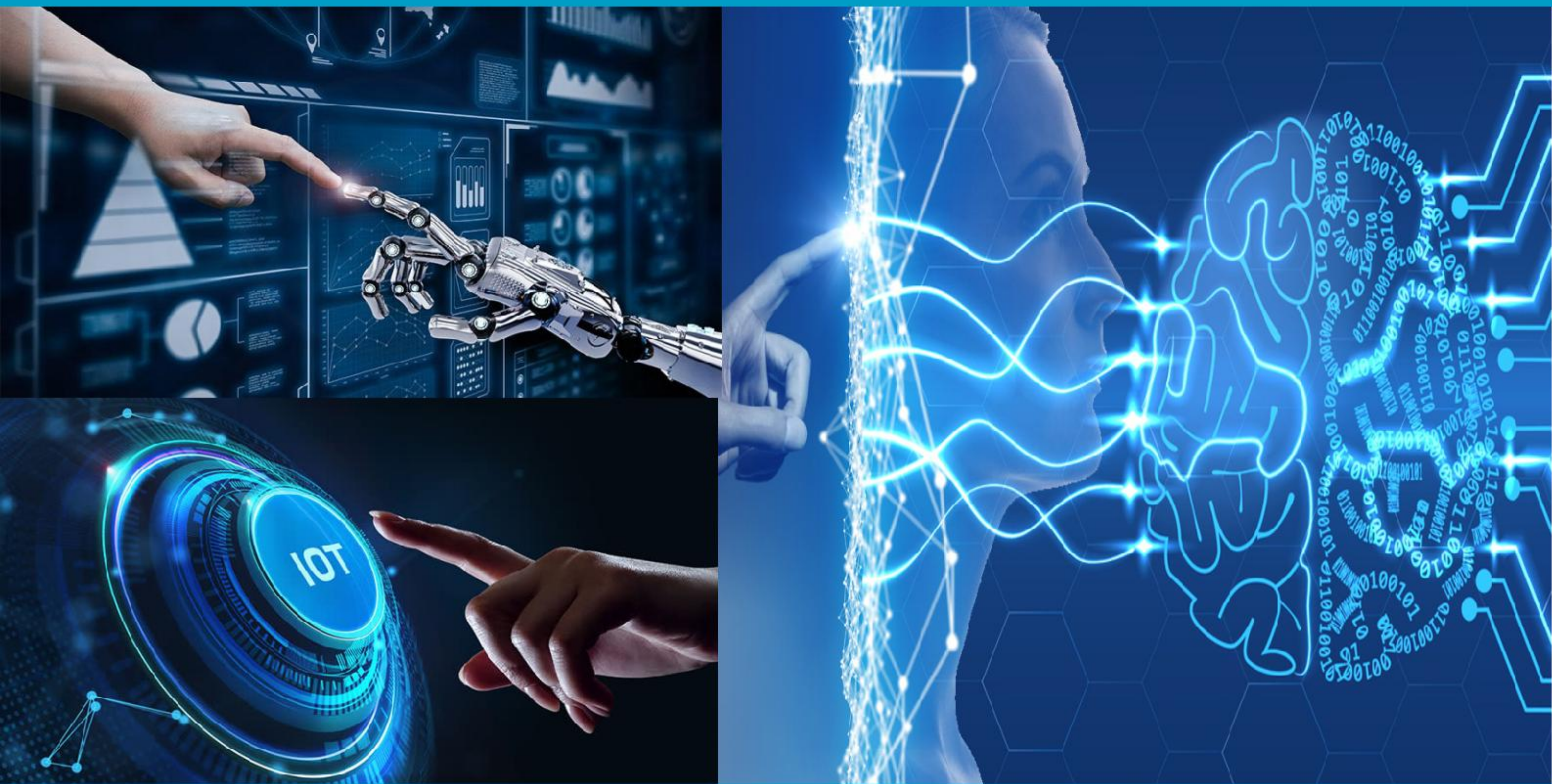

INTERNATIONAL JOURNAL OF MULTIDISCIPLINARY RESEARCH

IN SCIENCE, ENGINEERING, TECHNOLOGY AND MANAGEMENT

Volume 9, Issue 6, June 2022

INTERNATIONAL
STANDARD
SERIAL
NUMBER
INDIA

Impact Factor: 7.580

International Journal of Multidisciplinary Research in Science, Engineering, Technology & Management (IJMRSETM)

| ISSN: 2395-7639 | www.ijmrsetm.com | Impact Factor: 7.580|

| Volume 9, Issue 6, June 2022 |

| DOI: 10.15680/IJMRSETM.2022.0906040 |

An Experimental Study on the Characteristic's Laminar Separation on the Surface through Airfoil Elements

RAHUL KUMAR, ABHISHEK SINGHROHA,

A.P Mechanical Dept., CBS Group of Institutions, Haryana, India

MECHANICAL Engineering, CBS Group of Institutions, Haryana, India

ABSTRACT: The NACA0012 airfoil feature test approach was successfully investigated in this thesis. Analyzing the behavior of airfoils in this study required the use of an axial fan in the air tunnel. This kind of fan creates a pressure difference above and beyond the regulated zone for testing that is provided by the air tunnel. The ground level is not very high. The findings from the study on Airfoil Elements have been compared to standard data, and they have been determined to be compatible with those data. During this experiment, the NACA 0012 airfoil was subjected to four different speeds and four different attack angles. The end result was an overall lift coefficient of 12 degrees when the airfoil was subjected to an attack angle of +15 degrees. According to the theory and the results of the experiments, the stable angle of the airfoil should be 12 degrees. The fluctuations in the coefficient of drag cause the power consumption of the machine to experience a little amount of variance in the range of attack angles from -12 degrees to +12 degrees. If you want to run the machine with just a little bit more power, you'll see that the coefficient of lift lowers behind the table angle, which indicates that you'll need more power. When the attack angle is between -12 and +12 degrees, the lifting coefficient is rather high, but it drops off precipitously as the table angle rises. By using the Cp variation graph, this thesis is able to see pressure changes occurring on the airfoil surface.

KEYWORDS: Airfoil Elements, NACA0012 airfoil model, Wind Tunnel, CNC machine

I. INTRODUCTION

You may be asking why we decided to create a wind tunnel in this unconventional way. Or maybe a better question is, "Why the air tunnel?" The usage of wind tunnels to address aerodynamic difficulties may appear out-of-date in today's computer-driven environment. When compared to computers, which create enormous amounts of data, the airways give a unique flow visibility that may uncover crucial issues and remedies that can be recognized simply by numbers. For fluid-flexible designs, wind tunnels are a crucial tool for combining both kinds of data quickly and efficiently. To learn more about aerodynamics and the significance of airways, our project's primary goal is to teach us about the steps engineers use to investigate, assess, analyses, and, finally, solve societal issues of scientific and mathematical nature.
By building an air tunnel we hope to learn about aerodynamics, and, more often, about the process that engineers go through in the real world to explore ideas and solve problems. A common interest in aviation has led both of us to this project as we plan to explore the complex field of aviation engineering and have fun in this process, ultimately preparing us for future lessons, careers and real-life situations.

There is a boundary layer formed as the body changes from a solid state to a fluid one. The body is subjected to a variety of forces due to the existence of boundary layers. This is power

- The force of normal gravity
- Atmospheric thrust
- The force of drag
- The force of lifting

A person's biological fluids may be raised or lowered depending on how the air is pushed on their body.

II. EXPERIMENTAL SETUP

Experimental tests are performed in a liquid machine laboratory. Strategies used in current studies include measuring excess pressure. The NACA0012 airfoil model used for testing purposes was installed on a metal piece in the test

| ISSN: 2395-7639 | www.ijmrsetm.com | Impact Factor: 7.580|

| Volume 9, Issue 6, June 2022 |

| DOI: 10.15680/IJMRSETM.2022.0906040 |

section. The model had pressure ports along the center line throughout the chord that was connected to the manometer to measure local pressure through plastic tubes.

Wind Tunnel
There are several applications for air ducts in the study of fluid flow. Air tunnels have the benefit that testing may be done in a more controlled environment than in an open region.A low-speed subsonic air tunnel was employed in the present experiment. It's 8.03 since the test room's inlet area is 850 * 850mm and its cross section is 300 * 300mm. 660 * 660mm diffuser section with axial exhaust fan of 1300 RPM is available. Pitot tubes are used to determine the speed of the air inside the tunnel.The air tunnel used for testing is shown in Figure 1.

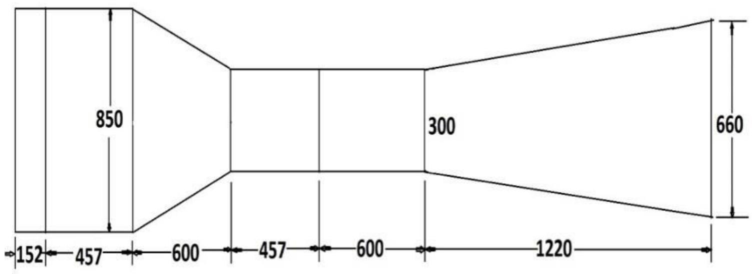

Figure 1: Line Diagram of Wind Tunnel

How it works
The reading of models or geometric forms is accomplished by inserting them into a perforated viewing pipe and fittings. In most cases, a system of fans is used to circulate air through the tunnel. Large air tunnels that are just a few meters wide need the deployment of a large number of smaller fans in order to produce sufficient airflow.Because the air tunnel in our present project was less subsonic, we simply employed one axial electric fan.Clean, laminar air is required for the tunnel's circulation. The turbulent air flow before reaching the test head was smoothed down by using neighboring PVC pipes of the lowest mesh size following this portion of the pipe.

Model
The NACA0012 airfoil was employed in the experiment. At 30% of the chord's length, the maximum thickness of the NACA0012 airfoil's 12-percent chord thickness is situated.

Figure 1 depicts the airfoil's form. The pressure holes are marked with two points.

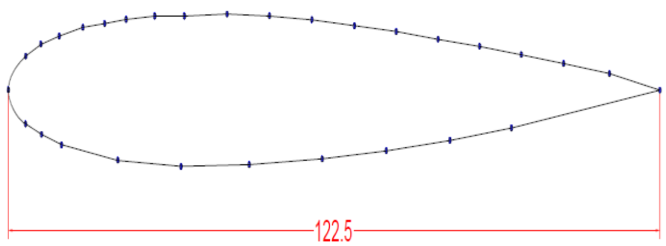

Figure 2: Its Pressure Ports are shown in this simple drawing of NACA 0012.

Fabrication of Models and Porting of Pressure
Acrylic is used to construct the model. A CNC machine was used to create the airfoil's aerodynamic shape. The CNC machine drilled 0.8mm wide pressure holes in the top and lower sections of the central component. There was a total of 29 pressure holes, with 15 holes positioned above and 12 holes located below the leading edge and the following. The front extremities of the top pressure holes are very flexible, allowing us to precisely distribute extra pressure. To link the pressure holes in the manometer to a 1.2 mm support tube, a hole with a diameter of 1.22 mm is drilled into the airfoil's front surface halfway down its length. A rubber tube connects the metal tubes to the manometer.

Because the sculpture is composed of three distinct components, the pieces are linked together by reacting chloroform with acrylic sheet to establish a bond.

| ISSN: 2395-7639 | www.ijmrsetm.com | Impact Factor: 7.580|

| Volume 9, Issue 6, June 2022 |

| DOI: 10.15680/IJMRSETM.2022.0906040 |

When using fine sandpaper with grit P400is size, the model's surface has a small roughness to it.
On the next page, you'll find a hole map file with the circumference of each pressure point measured in chord length units.

Port Map File

Table 1: Port Map File

Port no	X	Y	x/c	y/c
LE	0	0	0	0
U1	3.5	3.57	0.028	0.02856
U2	8.5	5.32	0.068	0.04256
U3	13.5	6.43	0.108	0.05144
U4	18.5	7.22	0.148	0.05776
U5	23.5	7.8	0.188	0.0624
U6	29.5	8.12	0.236	0.06496
U7	35.5	8.18	0.284	0.06544
U8	41.5	8.1	0.332	0.0648
U9	50.5	7.78	0.404	0.06224
U10	59.5	7.27	0.476	0.05816
U11	68.5	6.61	0.548	0.05288
U12	77.5	5.83	0.62	0.04664
U13	86.5	4.95	0.692	0.0396
U14	93.5	3.97	0.748	0.03176
U15	104.5	2.91	0.836	0.02328
TE	125	0	1	0
LE	0	0	0	0
L1	6.5	-4.41	0.052	-0.03528
L2	12	-5.62	0.096	-0.04496
L3	23	-6.36	0.184	-0.05088
L4	32.25	-6.82	0.258	-0.05456
L5	41.5	-7.2	0.332	-0.0576
L6	50.5	-7.23	0.404	-0.05784
L7	59.5	-7	0.476	-0.056
L8	68.5	-6.59	0.548	-0.05272
L9	77.5	-6.02	0.62	-0.04816
L10	86.5	-5.33	0.692	-0.04264
L11	95.5	-4.54	0.764	-0.03632
L12	104.5	-3.53	0.836	-0.02824
TE	125	0	1	0

Model Mounting

With a ball connected to the glass side and a metal component in the middle that permits center rotation and adjustment, the model is securely fastened to the air tunnel's inspection section. of volt. Both the left and right facades include eight-millimeter-diameter holes for inserting metal rods, which are then put into a bearing in the test chamber, which is centrally located in the test chamber. When the airfoil protector is installed, a model is supplied that may be adjusted to a desired air attack angle (see Figure 3).

| ISSN: 2395-7639 | www.ijmrsetm.com | Impact Factor: 7.580|

| Volume 9, Issue 6, June 2022 |

| DOI: 10.15680/IJMRSETM.2022.0906040 |

Figure 3: Airfoil Model Mounted in Tunnel Test Section

In order to change the model's angle, we simply loosened the screw, rotated it, and then tightened it again.

III. DATA ACQUISITION AND ANALYSIS

During testing, as air flows over the model, unstable pressure data at each pressure point must be obtained and stored for use during analysis to determine airfoil characteristics.In the process of obtaining the data after setting the required wind speed with the help of the controller pressure distribution study during the head is noted on the pressure distribution sheet. As our model has 29 more pressure ports of which 15 are over, 12 are at the bottom and 2 ports are leading and following behind. The upper bouts featured two cutaways, fore and aft; the upper bouts featured two cutaways, fore and aft.

Creo software detects a hole map file providing the position of all chord lengths while designing the input model. The model was created using this Creo file. Each hole's combination of X and Y was divided by the model's chord length to get the total number of measurements. Model characteristics were derived from a hole map file employed in a computation power that was applied to a model.

Test Configuration

We wanted to see how attack angle and Reynolds number affected airfoil characteristics in this test. Four different tests were run in order to complete this one. It's done by a number for each exam. Each test set has a distinct attack angle, ranging from -14 degrees to +15 degrees in a 2-degree climb. At the conclusion of each exam set, each test set is angled to make it easier to read.

Air tunnel collisions produce heat, which reduces density and leads to inaccurate findings. For this reason, each test set is completed over a prolonged period of time so that correct data may be obtained.

Below you'll find further information about each set.

1. In the first set of studies, a velocity of 9.82 m/s and a repeatability test of 6 degrees of attack were used, respectively.
2. 8.5 m/s was the speed at which the repeatability tests were performed at an attack angle of 8 degrees.
3. It was done at 7.76 m/s and the angle of attack was 6 for this third series of experiments and the test for repeatability.
4. 6.94 m/s and repeatability tests were performed for the fourth set of testing.

Data Analysis

The model's many attributes were calculated using raw data collected during data collection and kept on an Excel sheet.

The overall compression coefficient per pressure hole was first calculated in a systematic data analysis.

Calculation of Lift Coefficient

When the free constant pressure flowing through the model was removed and the impact of freestream variable head was removed, a neutral form of the pressure data known as the CP was developed. The lift force is calculated by adding the compression force and dividing it by the airfoil chord using the energy components perpendicular to the chord.

$$C_p = \frac{p_{local} - p_{static}}{\frac{1}{2}\rho U_\infty^2} = \frac{p_{local} - p_{static}}{p_{total} - p_{static}}$$

| ISSN: 2395-7639 | www.ijmrsetm.com | Impact Factor: 7.580|

| Volume 9, Issue 6, June 2022 |

| DOI: 10.15680/IJMRSETM.2022.0906040 |

$$C_n = -\oint C_p \, d\left(\frac{x}{c}\right) \approx -\sum C_p \, \Delta x/c$$

$$C_a = \oint C_p d\left(\frac{y}{c}\right) \approx \sum C_p \, \Delta y/c$$

$$C_l = C_n \cos\alpha - C_a \sin\alpha$$

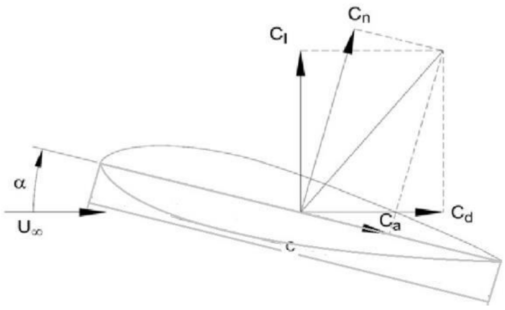

Figure 4: Figure illustrating Airfoil Forces Diagram

the raw information needed to calculate the coefficient of pressure at a speed of 9.82 m/s is provided in the following sheet

RUN NO.	1	2	3	4	5	6	7	8	9	10	11	12	13	14	15	16
AOA	-14	-12	-10	-8	-6	-4	-2	0	2	4	6	8	10	12	14	15
P0	30	29	28	27	26	26	26	25	24	24	23	22	21	21	21	20
Pinf	38	37	35	35	34	34	34	33	31	32	31	30	30	29	29	28
LE	45	45	56	50	42	34	29	25	24	24	24	27	30	30	24	24
U1	31	30	39	28	29	30	31	35	37	40	42	42	48	52	36	35
U2	33	32	31	31	31	32	33	36	37	38	40	40	46	48	36	35
U3	35	34	32	32	33	34	35	36	37	38	39	41	41	40	36	35
U4	36	35	33	33	33	35	35	36	37	37	38	40	39	38	35	35
U5	37	35	34	34	34	35	35	36	37	37	37	39	38	37	35	34
U6	37	35	34	34	34	35	35	36	36	36	36	37	37	36	34	34
U7	37	35	34	34	34	34	34	35	35	35	36	35	35	35	34	34
U8	38	36	35	35	35	35	35	36	35	35	36	35	35	34	34	34
U9	37	36	35	34	34	34	34	35	34	35	36	34	33	32	33	33
U10	37	35	34	34	34	33	33	35	34	34	32	32	32	31	33	33
U11	37	35	35	34	34	33	33	34	33	33	32	32	31	30	33	32
U12	38	36	35	34	34	33	33	34	33	32	31	31	31	30	33	32
U13	38	36	35	34	34	33	33	33	33	32	31	31	30	29	32	32

| ISSN: 2395-7639 | www.ijmrsetm.com | Impact Factor: 7.580|

| Volume 9, Issue 6, June 2022 |

| DOI: 10.15680/IJMRSETM.2022.0906040 |

U14	38	36	35	34	34	33	32	33	33	31	31	30	30	29	32	32
U15	39	36	35	34	33	33	32	33	32	30	30	29	29	28	31	31
TE	38	35	34	33	32	32	31	32	31	29	29	28	28	27	29	29
LE	45	45	56	50	42	34	29	25	24	24	24	27	30	30	24	24
L1	42	43	51	49	45	41	38	34	31	28	26	24	22	21	21	21
L2	43	44	50	47	43	40	38	35	32	30	28	26	25	23	24	23
L3	42	43	45	45	41	39	37	35	32	30	28	27	25	24	24	24
L4	43	43	42	42	41	39	37	35	33	31	29	28	26	25	25	25
L5	43	43	41	41	40	38	37	35	33	31	30	29	27	26	27	26
L6	43	43	40	40	39	38	36	35	33	32	30	29	28	27	27	27
L7	43	42	40	39	38	37	36	35	33	32	30	30	28	27	28	27
L8	43	41	49	38	37	36	35	33	32	31	30	29	28	27	27	27
L9	43	40	38	36	36	35	35	32	32	31	29	29	28	27	27	27
L10	43	40	37	36	35	34	35	32	31	30	29	29	28	27	27	27
L11	42	40	36	36	35	34	34	32	31	30	30	29	28	28	28	28
L12	42	40	36	35	35	34	34	32	31	30	30	29	28	28	29	28
TE	38	35	34	33	32	32	31	32	31	29	29	28	28	27	29	29

Calculation of Drag Coefficient

The force that opposes the movement of a moving item in respect to a liquid around it is known as "pull" in fluid dynamics (also known as "air resistance" or "liquid resistance"). Liquid and a solid surface may be separated by one or more layers of liquid (or regions). Gravity, in contrast to other opposing forces like the dry force, is speed dependent. Gravity always slows down the liquid in a liquid medium compared to the solid.

$$C_d = C_n \sin\alpha + C_a \cos\alpha$$

IV. RESULT AND DISCUSSION

For any study of test findings, the test/set method utilized for measurements must be validated first. Comparing airfoil papers from the NACA 0012 series is the first step in determining local pressure and aerodynamic coefficients.

C_p variation

These Cephalus are built against x / c with a certain attack angle.

x/c at 9.81m/s is depicted in the picture below to demonstrate how C p changes as a function of x/c

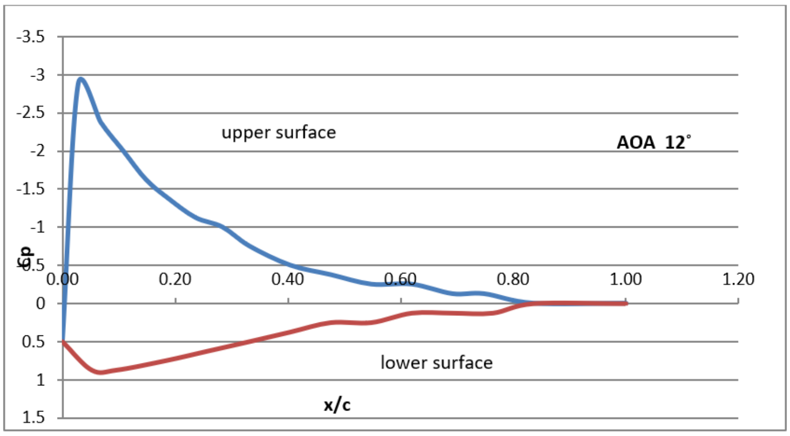

Figure 5: Variation of Cp vs AOA Graph

To illustrate, the graph indicates that at the leading edge, Cp has a positive value, which is followed by a negative value for the surface area, and then a positive value for the whole surface area. lift will be applied to the lower airfoil owing to the difference in pressure between the upper and the lower airfoil. A zero value for Cp indicates that there is no pressure difference between this end and the free streaming end.

International Journal of Multidisciplinary Research in Science, Engineering, Technology & Management (IJMRSETM)

| ISSN: 2395-7639 | www.ijmrsetm.com | Impact Factor: 7.580|

| Volume 9, Issue 6, June 2022 |

| DOI: 10.15680/IJMRSETM.2022.0906040 |

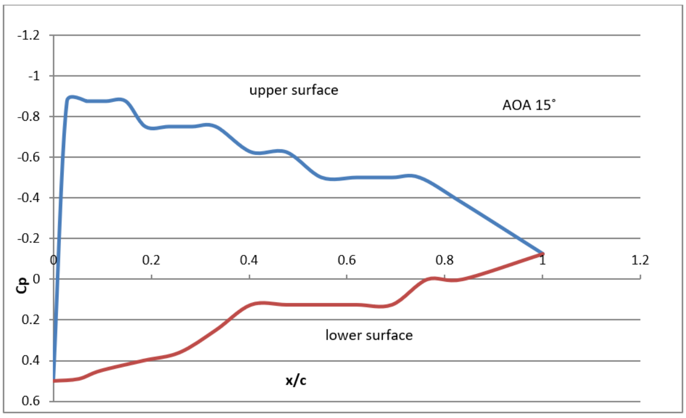

Figure 6: Cp vs AOA

To highlight how much of a difference there is between the airfoil at a 15-degree attack angle and one at a 14-degree attack angle, we've shown the Cp variation at that angle. In a shop, the airfoil receives the most pull strength with the least amount of lifting force.

At Reynolds Number, the Lift Coefficient Changes with Angle of Attack.

It is clear from Figure 5.4 that the sites are similar for small angles, but diverge at larger ones (above 70) as the Reynolds number increases. Increasing the attack angle weakens the flow's capacity to combat the large negative gradients, allowing it to break the consecutive limit and flow out of control. Freestream turbulence rises with Reynolds incoming flow rate, causing the boundary layer to have a turbulent kinetic force, allowing it to remain attached for a longer distance than in the case of a lower Reynolds number. At high attack angles, the lifting coefficient is somewhat lower than the minimum number of Reynolds because of this separation of flow into subdivisions.

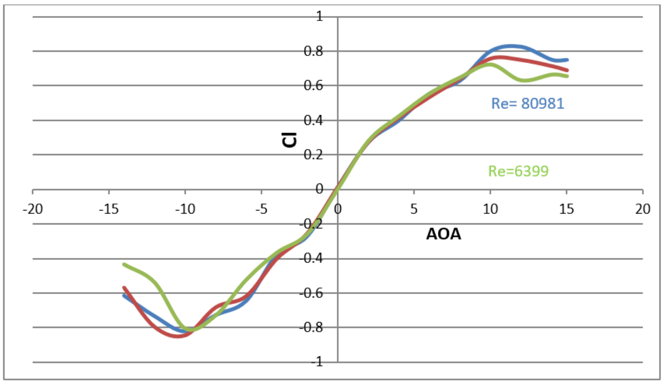

Figure 7: C_l Versus A Plot at Different Reynolds Numbers

| ISSN: 2395-7639 | www.ijmrsetm.com | Impact Factor: 7.580|

| Volume 9, Issue 6, June 2022 |

| DOI: 10.15680/IJMRSETM.2022.0906040 |

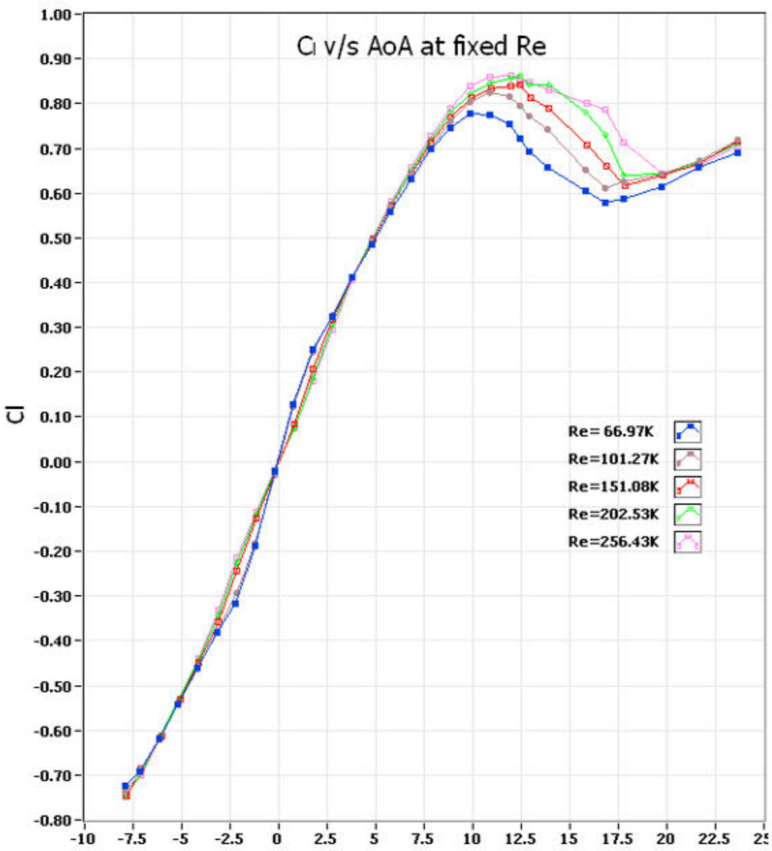

Figure 8: Reference Data

When looking at Figure 5.4, it is clear that tiny angles (less than 70 degrees) are followed by the sites, whereas larger angles (greater than 70 degrees) begin to vary. Inability to overcome the negative high slopes breaks the consecutive limit as the attack angle rises. Since freestream turbulence rises in proportion to Reynolds incoming flow rate, so does the boundary layer's kinetic energy, making it stickier over longer distances than it would be under conditions of low Reynolds number. At high attack angles, the lift coefficient is somewhat lower than the low Reynolds number because of this separation flow separation.

Figure 4.8 shows the fluctuation in lifting coefficient with a constant attack angle and Reynolds inflow number. Clear evidence that Cl differs just little may be found. The length of the plateau on the Cp profile is shortened when the invasion angle is low (between 0° and 5°). As a consequence, a rise in Re induces a minor drop in Clavules. Higher angles, bring the bubble, resulting in a larger suction area. In these circumstances, the flow becomes more erratic as the number of Reynolds increases, and this is why there is an increasing trend in the number of Reynolds.

V. CONCLUSION AND FUTURE WORK SCOPE

The liquid machinery laboratory successfully used the NACA0012 airfoil feature test procedure. An axial fan in the air tunnel, which offers a controlled region for testing and produces a pressure differential above and beyond, was employed to analyses airfoil behavior in this work. The ground level is rather low.

Results from the Airfoil Elements research have been compared to standard data and found to be consistent.

The study's findings are outlined below.

- There were four distinct speeds and four different attack angles for the NACA 0012 airfoil in this experiment, which resulted in an overall lift coefficient of 12 degrees at an attack angle of +15 degrees. The airfoil's stable angle should be 12 degrees, according to both tests and theory.

- There is a little fluctuation in the machine's power consumption in the range of attack angles from -12 to +12, according to the coefficient of drag variations.
- To operate the machine with a slight increase in power, the coefficient of lift drops behind the table angle indicating the need for further power.
- The lifting coefficient is high in the attack angle range of -12 to +12, but it decreases as the table angle increases.
- We can see pressure variations on the airfoil surface using the Cp variation graph.

REFERENCES

[1] Y. Lian, and W. Shyy, "Laminar-Turbulent Transition of a Low Reynolds Number Rigid or Flexible Airfoil", AIAA Journal, Vol. 47, No. 7, 2007.
[2] George Phlip, "An experimental study on the characteristics laminar separation on the surface"
[3] http://www.mh-aerotools.de/airfoils/methods.htm
[4] http://www.wikipedia.com
[5] N Gregory, and C L O'reilly, "Low speed characteristics of NACA 0012 Airfoil Section including the effects of Upper Surface Roughness Simulating Hoar Frost" report by Ministry of Defence.
[6] Charles Holicker, "Characteristics of NACA 0012 Wing: Determination of Cl and Cd using foce Balance"
[7] Mohsen Jahanmiri, "Laminar Separation Bubble: Its Structure, Dynamics and Control", research report 2011/06
[8] http://www.aerolab.com
[9] http://www.century-of-flight.com
[10] Selig, "Wind Tunnel Testing Airfoils at Low Reynolds Nombers", 49thAIAA Aerospace Sciences Meetin